Astron. Astrophys. 349, 267–275 (1999)

ASTRONOMY AND ASTROPHYSICS

The chemical composition of the silicate dust around RAFGL7009S and IRAS 19110+1045⋆

K. Demyk[1], **A.P. Jones**[1], **E. Dartois**[2,1], **P. Cox**[1], **and L. d'Hendecourt**[1]

[1] IAS-CNRS, Université Paris XI, Batiment 121, F-91405 Orsay Cedex, France
[2] IRAM, 300, rue de la Piscine, F-38406 Saint Martin d'Hères, France

Received 18 March 1999 / Accepted 30 June 1999

Abstract. We have studied the chemical composition of the silicates around the two massive protostellar objects RAFGL7009S (IRAS 18316-0602) and IRAS 19110+1045. The silicate features of both sources are similar. The position and shape of the 9.6 and 18 μm silicate bands coincide with those of amorphous pyroxene-type silicates. We find that the silicate features cannot be reproduced with compact pyroxene grains containing magnesium and iron. An admixture of iron, aluminium and some degree of porosity is necessary to reproduce respectively the red wing of the 18 μm band, the plateau between the two silicate bands and the widths of the bands. The iron is to be found in the form of Fe-rich pyroxenes, also containing small amounts of calcium, and in iron-oxides. Better fits are obtained with aluminium incorporated into the silicate structure (in aluminosilicates) than for aluminium in oxides such as Al_2O_3. The compositions we propose are in agreement with cosmic elemental abundance constraints. No crystalline material is observed in either source and we find that at most 1–2% of the silicate mass could be crystalline in these sources.

Key words: infrared: ISM: lines and bands – molecular processes – ISM: abundances – ISM: dust, extinction – ISM: molecules – ISM: individual objects: RAFGL7009S – ISM: individual objects: IRAS 19110+1045

1. Introduction

Silicates are to be found in most regions in space. They are formed in the circumstellar shells around evolved oxygen-rich (O-rich) stars and injected into the ISM via stellar winds (e.g. Gehrz 1989). After passage through the diffuse medium where they may undergo various structural modifications, they are incorporated into molecular clouds. The collapse of these clouds will then incorporate them into the regions around protostars and into (proto) planetary systems. Silicates around protostars are thus old. They have likely been highly processed by interactions with stellar winds, cosmic rays, photons, by gas-grain and grain-grain collisions in shocks in the ISM (e.g. Barlow 1978a,b). The processing of dust grains alters their physical and chemical properties and the coagulation of grains in dense regions can lead to porous structures. Dust around protostars may then be different from the newly formed dust around evolved stars and from the dust in the ISM. Although the ISO satellite has revealed the presence of crystalline silicates around some evolved stars (Waters et al. 1996, 1998) and young disk-like stars (Waelkens et al. 1996, Malfait et al. 1998), the silicates around massive protostars such as W33 A or NGC7538 IRS9 are known to be highly amorphous (Willner et al. 1982). The lack of any structure in the 9.6 and 18 μm bands makes it difficult to determine precisely the composition of the silicates around protostars. However, the studies of Jäger et al. (1994) and Dorschner et al. (1995) show that the peak positions of the silicate bands around protostars are compatible with pyroxene-type silicates containing iron and traces of calcium.

Silicate grains are composed of the highly depleted elements Mg, Fe and Si, but Al, Ca, Na should also be present in oxides or in the silicate structure. Gas phase molecules containing various metallic atoms (except iron) have been detected (Ziurys et al. 1995, Guélin et al. 1993) but the column densities involved are several orders of magnitude below those expected from the cosmic abundances of the elements. Serra et al. (1992) proposed that iron, or more generally metallic atoms, could be bound to PAH molecules in organometallic species. Such a population of metal-PAH molecules could explain ∼5–10% of the depletion of metal atoms in the diffuse ISM (Klotz et al. 1995). However there is to date no observational evidence for the existence of such molecules in the ISM. It is thus generally believed that all the "missing" metal atoms are locked up in dust grains. Iron, a highly depleted species, could be incorporated into grains as oxides, metallic iron or within the structure of the silicates. Jones et al. (1996) showed that, because metallic iron grains are dense they are accelerated to high velocities behind shock waves and easily destroyed, their lifetime is therefore shorter than that for silicate or graphite grains. Also, pure iron grains should be oxidized in the ISM by interactions with the gas phase species on times scales of the order of 10^6 yr in the diffuse ISM (Jones 1990). Savage & Sembach (1996) discussed the presence of Fe either in oxides or in silicates in view of the observed de-

Send offprint requests to: K. Demyk (demyk@ias.fr)

⋆ Based on observations with ISO, an ESA project with instruments funded by ESA Member States (especially the PI countries: France, Germany, the Netherlands and the United Kingdom) and with the participation of ISAS and NASA.

pletion patterns in the halo and in warm clouds. Halo cloud depletions give the composition of the core of the grains (the most refractory part) and the difference between halo and cool cloud depletions gives that of a less refractory layer (mantle). They conclude that the grain core should be composed of Mg-Fe-silicates mixed with oxides while the mantle should only contain Mg-Fe-silicates.

Silicates could also contain aluminium as it is highly depleted in the gas phase (e.g. Mutschke et al. 1998). Aluminium oxide Al_2O_3 is believed to be one of the first condensation products around evolved stars where silicate formation occurs (Nuth 1996, Sedlmayr 1989, Jones 1990). It has been proposed to explain the 13 μm band in oxygen-rich stars (Begemann et al. 1997). Aluminium can also be directly incorporated into the structure of silicates, in aluminosilicates (e.g., Mutschke et al. 1998). Howk & Savage (1998) report observations of the depletion of aluminium around late-O/early-B stars which imply that dust in the nebulae around these objects contains some aluminium. However they do not specify in which form it should be present.

The ISO observations are particularly well-adapted to the study of silicates. Firstly, the large wavelength coverage permits a simultaneous study of the silicate stretching and bending modes and a precise determination of the continuum. Secondly, thanks to the high resolution a study of the band shapes is possible. Using the optical constants of silicates, aluminosilicates and oxides of the Jena Group (Mutschke et al. 1998, Jäger et al. 1994, Dorschner et al. 1995, Begemann et al. 1995) we have modeled the silicate absorption of the massive protostellar objects RAFGL7009S (IRAS 18316-0602) and IRAS 19110+1045 (hereafter IRAS 19110). The model is described in Sect. 3. Results are presented in Sect. 4. We discuss in Sect. 5 the nature of the silicates in protostellars objects and Sect. 6 is devoted to the derived dust abundances in the two sources. Sect. 7 focusses on the silicate evolution by comparing the spectral characteristics of silicates around protostars with those of silicates around evolved stars and in the ISM. Finally, in Sect. 8 we derive an upper limit to the crystalline silicate component that could be present in the two protostars.

2. ISO SWS and LWS spectra

Figs. 1 and 2 present the combined SWS and LWS spectra of the protostellar objects RAFGL7009S and IRAS 19110+1045, respectively (see Dartois et al. 1998a for information about the data reduction). In both spectra we observe dominant bands at 9.6 and 18 μm due respectively to the Si-O stretching and O-Si-O bending vibrations in amorphous silicates. In addition, numerous bands due to ices are also seen (H_2O, CO, CO_2, CH_3OH, CH_4, d'Hendecourt et al. 1996, Dartois et al. 1998a). In RAFGL7009S the 9.6 μm band is saturated, indicating that this object is deeply embedded. Indeed water ice is about twice as abundant in RAFGL7009S as in IRAS 19110. In both sources the 9.6 μm band has a shoulder at $\sim$11–12 μm due to the libration mode of water ice. The CO_2 bending mode at 15.2 μm is superimposed on the 18 μm silicate band. The red wing of the

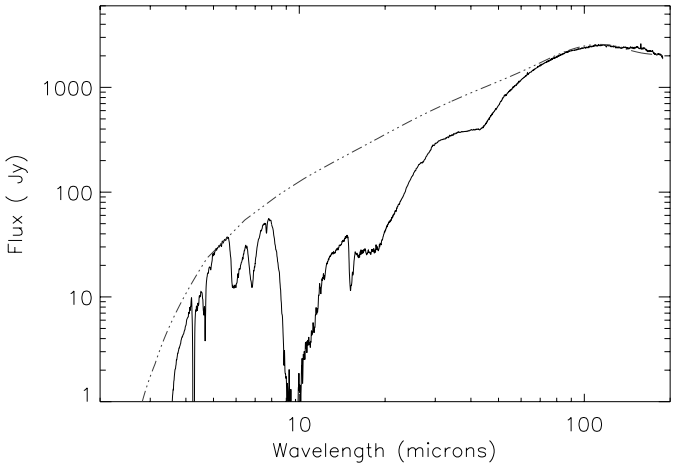

Fig. 1. The combined SWS and LWS spectrum of RAFGL7009S (from Dartois et al. 1998a) with the adopted continuum.

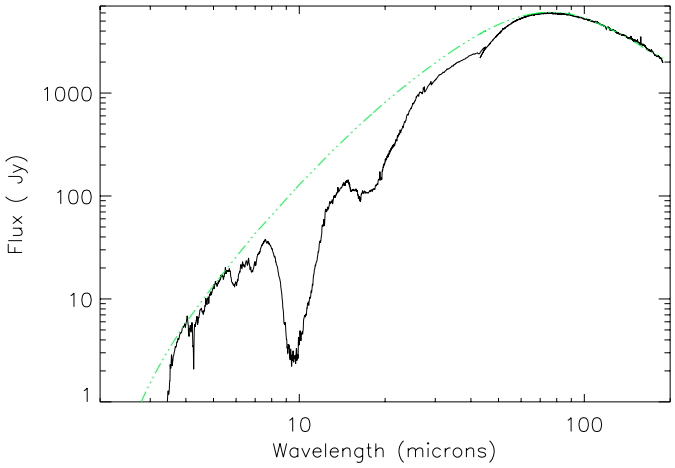

Fig. 2. The combined SWS and LWS spectrum of IRAS 19110+1045 (from Dartois et al. 1998a) with the adopted continuum.

18 μm band is interesting because it shows a weak and broad bump at $\sim$22–23 μm which is absent in the laboratory spectra of silicates and in most silicate observations. Effects due to the continuum subtraction were studied by adopting several extreme continua. The continua were determined using a cubic spline assuming that the 4–5 μm and the 50–200 μm regions give the continuum level. These continua are due to the infrared emission from the dust heated by the UV radiation of the newly-formed stars. The choice of the continuum induces variations only in the blue wing of the 10 μm band and in the continuum level at $\lambda \geq 25$ μm and these variations do not exceed 10%. The continua adopted in this paper are shown as dotted-dashed lines in Figs. 1 and 2.

3. Modelling

We have performed Effective Medium Theory and Mie calculations (Bohren & Huffman 1983) to derive the extinction caused by spherical grains containing different amounts of vacuum and oxides. No size distribution was adopted because we study

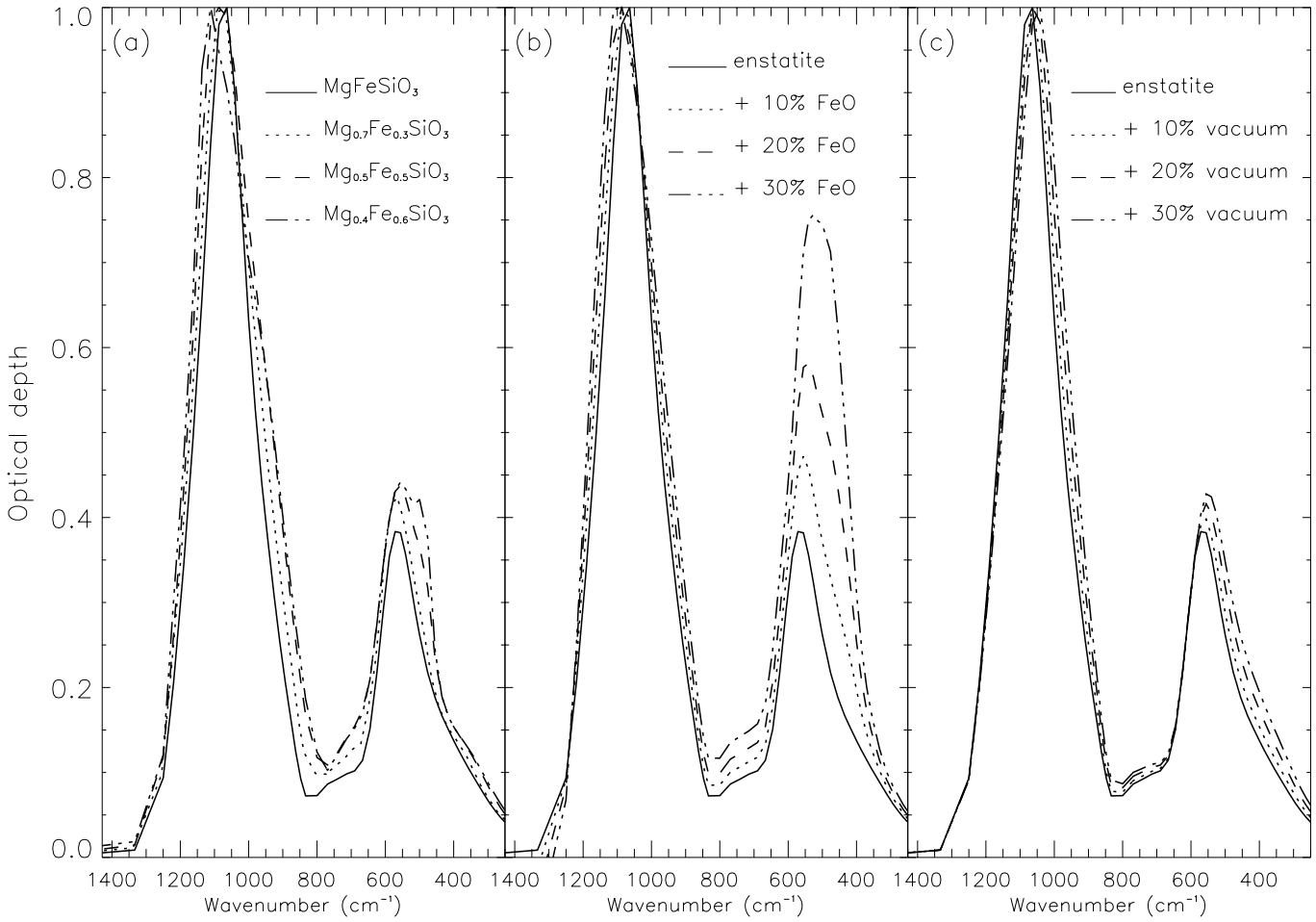

Fig. 3a–c. Influence of **a**: the presence of iron in pyroxenes, **b**: the presence of iron-oxide inclusions in an enstatite grain, **c**: porosity in an enstatite grain. The spectra are normalized to unity for comparison.

grains in the Rayleigh limit (i.e. grain radius $\ll \lambda$). We have adopted a grain size of 0.2 μm, which is justified by the good laboratory fits to the ice bands (e.g. the 7.7 μm CH_4 band, Dartois et al. 1998b), which show that there is no scattering effect and that the grains are thus small compared to the wavelength. At the wavelengths of interest (10–30 μm), pure absorption dominates the spectrum. Consequently we can directly compare the models with the observations once the continua have been substracted.

There are several ways to study the influence of the presence of different materials on the propagation of light, depending on how these materials are incorporated in the grains (assuming they are not in different grain populations). We have used the Maxwell-Garnet theory to calculate the average dielectric constant of an inhomogenous mixture composed of spherical inclusions (vacuum or solid) uniformly embedded in a homogeneous matrix. This average dielectric constant is then used in Mie calculations to derive the dust extinction. Mie theory can also be applied to calculate the extinction of coated grains (spherical or ellipsoidal). Such a segregation in the grains has been proposed by Savage & Sembach (1996). However, as pointed out by Jones (1988), using these theories, it is impossible, for a two-component mixture, to discriminate between the different structures in the infrared.

Fig. 3a shows the spectral influence of the concentration of iron in pyroxene ($Mg_xFe_{1-x}SiO_3$). The results are identical to those found by Dorschner et al. (1995). Models of coated spheres with FeO cores and pyroxene mantles or of oxides uniformly mixed with pyroxene (the two models are indistinguishable in the infrared) show that the presence of FeO strongly diminishes the 10/18 μm band ratio as the FeO band at $\sim 20\,\mu$m (500 cm^{-1}) becomes more and more pronounced (Fig. 3b). It also broadens both the 10 and 18 μm bands and shifts them towards shorter and longer wavelengths respectively. These results are in agreement with CDE calculations of Henning et al. (1995).

We have also investigated the influence of porosity on extinction. Vacuum is incorporated into the grains as small spherical inclusions in the Effective Medium Theory calculations. It increases the FWHM of both the 10 and 18 μm bands (Fig. 3c), shifts both bands towards longer wavelengths and reduces the 10/18 μm band ratio.

4. Results

4.1. Ice mantle

In order to compare the models with the observed spectra, we have added ice absorption, consistent with that observed, to the silicate features. For RAFGL7009S we added H_2O, CO_2 and CH_3OH ices with the abundances previously derived by d'Hendecourt et al. (1996) and Dartois et al. (1999). We did not consider molecules such as CH_4 and CO (present in the ices around RAFGL7009S) as they have no infrared active vibrations in the 8–35 μm range. Only H_2O and CO_2 ices were added for IRAS 19110 with the abundances derived by Dartois et al. (1998a).

4.2. RAFGL7009S

In RAFGL7009S the Si-O stretching vibration of silicates falls at 9.6 μm and is very broad (FWHM of 2.35 μm after the ice absorptions have been subtracted). The lower limit to the 10/18 μm band ratio is 2.15. As can be seen in Fig. 4, olivine clearly does not fit the protostellar spectrum: the bending mode falls too short in wavelength (17.2 μm), the 10/18 μm band ratio is too low and both bands are too narrow. This holds for all values of the Fe/Mg ratio. A mixture of pyroxene and olivine could reproduce the 10 μm band but not the 18 μm band: the band peaks at too short wavelength and the red wing is not reproduced. We conclude that amorphous olivine is not an important constituent of the silicates around this object. Furthermore, as the 10/18 μm band ratio for an olivine-pyroxene mixture is too small, an admixture of vacuum or iron oxide will further diminish this ratio. The positions of the pyroxene bands are in better agreement with the observed bands. However, spherical pyroxene grains without oxide or vacuum inclusions, do not provide a good match to the protostellar spectrum because both the 10 and 18 μm bands are too narrow. We have considered simple pyroxenes ($Mg_xFe_{1-x}SiO_3$) and pyroxenes containing traces of calcium and aluminium (Henning & Mutschke 1997), hereafter called "cosmic" silicates because their composition (Mg 28.1%, Fe 17.3%, Al 1.1%, Ca 2.2% and Si 51.3%) closely resembles the cosmic elemental abundances.

The vibrational modes of amorphous minerals in the mid-infrared (MIR) are usually not unequivocal. We find several good fits to the silicate features of RAFGL7009S that agree with cosmic abundance constraints (Fig. 5, Table 1). The silicate features in RAFGL7009S are well reproduced with Mg-Fe-pyroxene grains, with a Fe/Mg ratio in the range of 0.4–0.65, containing ∼5% (by volume) of FeO and ∼15% of vacuum (Fig. 5). The "cosmic" silicates reproduce very well the blue wing of the 10 μm band whereas $Mg_xFe_{1-x}SiO_3$ silicates peak at slightly shorter wavelengths. Furthermore the 10 μm band in "cosmic" silicates is broader allowing a better fit to the observed bands. Good fits can also be found with populations of aluminosilicate grains and "cosmic" pyroxene grains. The presence of aluminium gives rise to absorption at $\sim$700cm^{-1}. It is difficult to find a reasonnable fit with Al_2O_3 incorporated into the cosmic silicates because it diminishes the 10/18 μm band ratio.

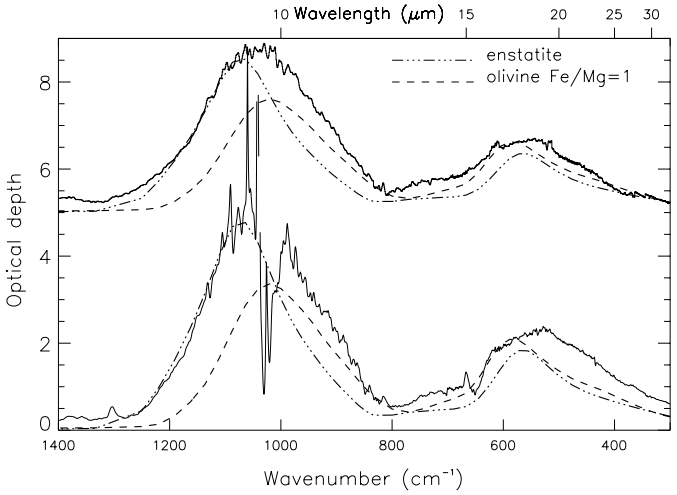

Fig. 4. Comparison of the silicate features of RAFGL7009S (lower spectrum) and IRAS 19110 (upper spectrum) with models of spherical grains of enstatite and olivine. The continua and the ice absorptions have been subtracted. The strong noise at $\sim$9 μm in RAFGL7009S is due to the saturation of the stretching silicates band, the feature at $\sim$650 cm^{-1} is due to a slight shift between the CO_2 laboratory spectrum and the observations.

Table 1. Abundance of elements of the refractory phase in RAFGL7009S and IRAS 19110

	Dust phase abundance			RAFGL 7009S		IRAS 19110	
	(1a)	(1b)	(2)	a	b	c	d
Si	100	100	100	100	100	100	100
Fe	94	86	158	68	51	56	51
Mg	108	104	111	52	55	60	53
Al	$\sim10^{(3)}$	$\sim10^{(3)}$	$\sim10^{(3)}$	13	0	17	10
O	1323	809	741	346	317	367	311
Ca	-	-	-	2	4	3	2

(1): Savage & Sembach (1996) a: with respect to solar abundances, b: with respect to B-stars abundances
(2): Snow & Witt (1996)
(3): Mutschke et al. (1998)
(a): cosmic pyroxene grains with 15% of vacuum and 10% of FeO (the percentage are by volume). and aluminosilicates grains ($Mg_4Fe_4Al_2Si_8O_{27}$) with 5% of FeO. (b): cosmic pyroxene grains with 5% of FeO and 15% of vacuum. (c): cosmic pyroxene grains with 3% of FeO and 15% of vacuum. and aluminosilicates grains ($Mg_2Fe_2Al_2Si_4O_{15}$). (d): cosmic pyroxene grains with 3% of FeO and 15% of vacuum. and aluminosilicates grains ($Mg_4Fe_4Al_2Si_8O_{27}$) with 15% of vacuum.

However one cannot exclude that part of the aluminium is in the form of Al_2O_3. The appearent feature at 16 μm (625 cm^{-1}) is not reproduced in our fits. This may simply be an artefact due to an overlap of two SWS AOT bands at 16 μm.

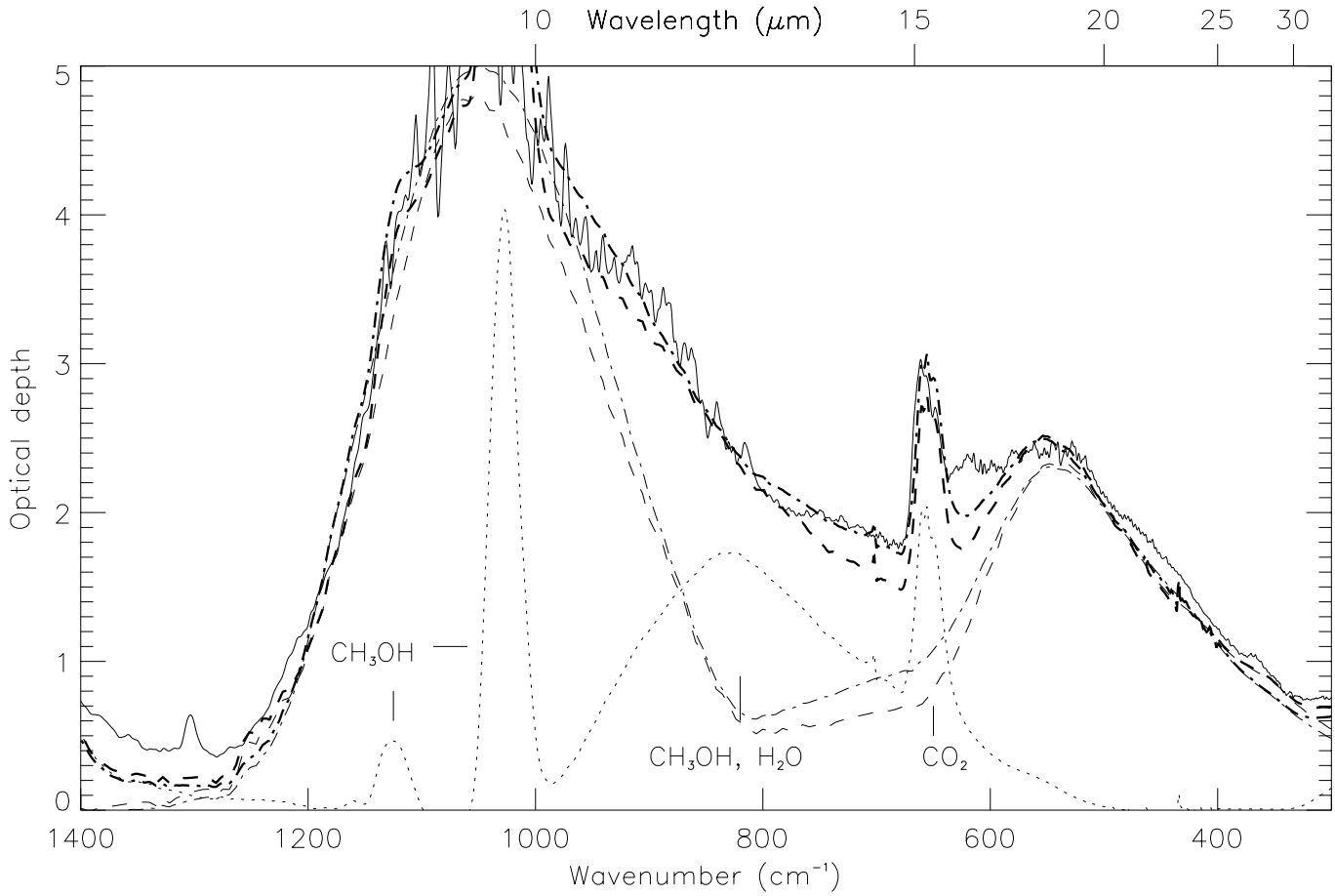

Fig. 5. Comparison of the ISO-SWS01 spectrum of RAFGL7009S (the continuum has been subtracted) with models of spherical oxide-silicate grains. Long dashed line: cosmic pyroxene grains with 15% of vacuum and 5% of FeO. Dotted-dashed line: mixture of two grains populations, one of cosmic pyroxene grains with 15% of vacuum and 10% of FeO and the other of aluminosilicate grains ($Mg_4Fe_4Al_2Si_8O_{27}$) with 5% of FeO. The thin lines represent the silicate models and the thick ones the model plus the ice absorptions. The dotted line represent the ice spectrum we added to the silicate models.

4.3. IRAS 19110

The Si-O stretching mode in IRAS 19110 is very similar to that of RAFGL7009S. It peaks at 9.6 μm and has the same FWHM, once the ices have been subtracted and the bands have been normalised at 10 μm. However, the bending mode and the plateau between the two modes are slightly different. IRAS 19110 has a more pronounced plateau in the 12–16 μm region while the red wing of the bending mode occurs at shorter wavelengths than in RAFGL7009S (Fig. 6). The 10/18 μm band ratio is equal to 2.2, similar to that of RAFGL7009S.

As in the case of RAFGL7009S, it is not possible to obtain a good fit to the silicate features of IRAS 19110 with compact grains of olivine, pyroxene or pyroxene-olivine mixtures (Fig. 4). We have found several fits but most of them require more aluminium than the cosmic abundance (Table 1) in order to match the strong 12–16 μm plateau. The best fits to IRAS 19110 require two grain populations. One of cosmic pyroxene with about 15% of vacuum and few percent of FeO ($\sim$3%) and the second of aluminosilicates, $Mg_2Fe_2Al_2Si_4O_{15}$ or $Mg_4Fe_4Al_2Si_8O_{27}$ with about 15% of vacuum (Fig. 6 and Table 1). However, the best fits contain too much aluminium and fits with less aluminium are poorer. As discussed above, the discrepancy in the 600 and 650 cm^{-1} region ($\sim$ 16 μm) may not be real.

5. Nature of the inclusions and silicates

We have considered inclusions of FeO because it is the simplest iron oxide. Its formation has been studied by Begemann et al. (1995). Iron can also be oxidised in the form of hematite (Fe_2O_3) or magnetite (Fe_3O_4). Molecules of these species have been proposed as the first nucleation sites on which silicate grains grow (Nuth & Hecht 1990). It could be possible to discriminate between different types of inclusions by observing in the near-IR/visible wavelength range because inclusions will alter the opacity differently according to their composition (Ossenkopf et al. 1992). Unfortunately, this wavelength range is difficult to access in such highly extinguished massive protostars. Inclusions of metallic iron are unlikely because Fe is easily oxidised and silicates provide an oxidising environment. However, in stars with rapidly cooling outflows, silicates could be oxygen-

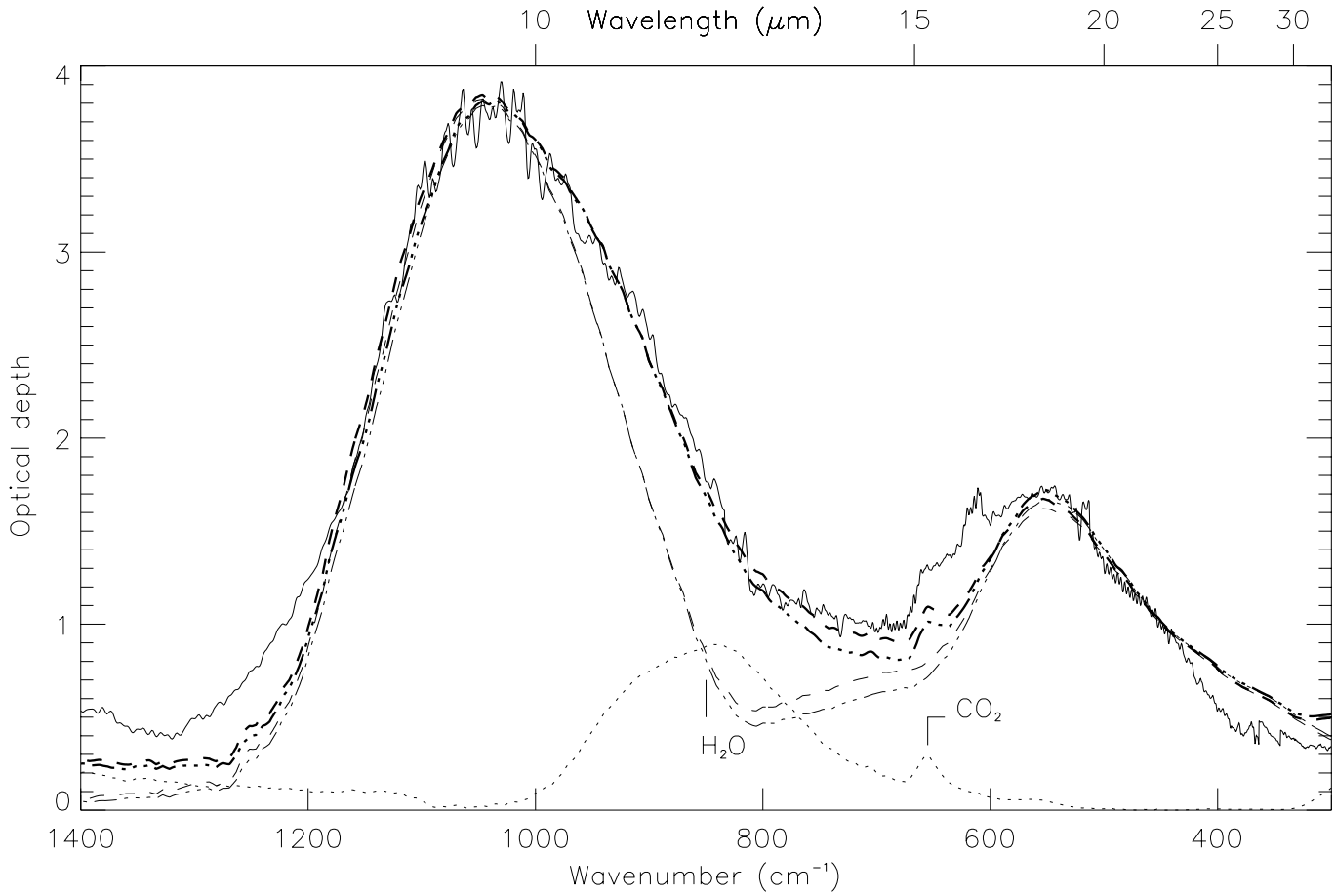

Fig. 6. Comparison of the ISO-SWS01 spectrum of IRAS 19110 (the continuum has been subtracted) with models of spherical oxide-silicate grains. Long dashed line: two grains populations, one of cosmic pyroxene grains with 3% of FeO and 15% of vacuum and the other of aluminosilicate grains ($Mg_2Fe_2Al_2Si_4O_{15}$). Dotted-dashed line: two grains populations, one of cosmic pyroxene grains with 3% of FeO and 15% of vacuum and the other of aluminosilicate grains ($Mg_4Fe_4Al_2Si_8O_{27}$) with 15% porosity. The thin lines represent the silicate models and the thick ones the models plus the ice absorption. The dotted line is the ice spectra we added to the silicate models.

deficient leading to the presence of pure Fe inclusions (Nuth & Hecht 1990). If these inclusions are deeply embedded in the silicate matrix they would be prevented from oxidation in the ISM. Indeed Fe-Ni alloys have been found in chondritic IDPs (Bradley et al. 1988). Metallic iron has no active vibrational modes in the MIR and would be impossible to detect in this wavelength range. Finally iron could also be found in troilite (FeS) as Fe-rich sulfide grains have been found in chondritic IDPs (Bradley et al. 1988). However observations of sulfur depletions are uncertain and show that 0 to 75% of the cosmic sulfur could be in the refractory dust (Pollack et al. 1994) with a 0% value usually adopted in dust models. Because the quantities involved are small (typically a few percent) we believe that the use of hematite, magnetite or metallic iron would not have greatly changed the spectra in the MIR region nor the abundances we derived for the dust elements.

We have obtained better fits with aluminium incorporated into the silicate structure rather than in the form of Al-oxides. However, from our data we cannot exclude the possiblity that Al-oxides could be present in the grains around both protostars. If aluminosilicates are present in dust grains, how and where are they formed? Are they directly produced in the envelopes around evolved stars or do they result from the chemical and physical processing of pyroxene or olivine silicate grains containing aluminium oxides? Al-oxides have been proposed to be the primary condensation product from which the silicate grains formed (Stencel et al. 1990, Nuth 1996). In this case, aluminium should be present in the grain in the form of Al-oxide inclusions. On the other hand, experiments on the condensation of SiO_x-AlO_x and SiO_x-AlO_x-FeO_x smokes show that aluminium is incorporated into a silicate structure either in Al-silicates similar to kaolinite and halloyte or in Al-Fe-silicates (Nuth 1988, Rietmeijer & Nuth 1990). It is thus probable that both aluminium oxides and aluminosilicates are present in the grains. A combination of aluminosilicates (Mg-Fe-Al-silicates) and Al_2O_3 have been proposed by Mutschke et al. (1998) to reproduce spectra of the two stars IK Tauri and EP Aquarii.

As seen before, the presence of iron oxides in silicate grains broadens the bands. However the amount of oxide is constrained by the red wing of the 18 μm band and with this constraint,

it cannot reproduce the width of the protostellar bands. The addition of about 15% (by volume) of vacuum is needed to fit the spectra of both sources. The large widths of the silicate bands in the spectra of protostars indicate that the grains around these objects are either coagulated grains or that they became chaotic under the effects of processing. As porosity in grains is a natural consequence of coagulation, the necessity to add vacuum in our model could indicate that some grain coagulation occured in the dense cloud prior to star formation.

6. Dust phase abundances

The column density of silicon necessary to reproduce the silicate bands is 5.7–11.2$\times10^{18}$ cm^{-2} for RAFGL7009S and 5.1–5.6$\times10^{18}$ cm^{-2} for IRAS 199110. Note that the large uncertainty for RAFGL7009S is due to the saturation of the 10 μm silicate band which relaxes the constraints on the models. By modeling the spectral energy distribution of IRAS 19110, Hunter (1997) and Hunter et al. (1997) have determined the hydrogen density in this source to be N_{H_2} $\sim$7.0$\times10^{23}$ cm^{-2}. This implies that 3.6–4 Si atoms per 10^6 H atoms are needed to fit the spectrum. This is well below the constraints for all reference cosmic abundances (Table 1) (Savage & Sembach 1996, Snow & Witt 1996). The situation is less clear for RAFGL7009S for which the hydrogen column density is determined with a large uncertainty. Mc Cuthcheon et al. (1995) derived the hydrogen column density in RAFGL7009S by two methods and found N_{H_2} $\sim$ 1.7–9.8$\times10^{23}$ cm^{-2}. Thus 5 to 32 Si atoms per 10^6 H atoms are required in the dust phase in our models. The upper limit is in agreement with solar reference abundances (Savage & Sembach 1996) but in excess of the B star reference and the reference abundances of Snow & Witt (1996). However, the discrepancy is less than a factor two and if we take the average of the given H_2 column densities our models meet the abundance constraints.

If we assume that all of the Si atoms in our sources are in silicates, then we can compare the relative abundances of the elements contained in the refractory dust phase with respect to Si. Values of the dust phase abundances depend on the chosen reference abundance. Savage & Sembach (1996) give the overall abundance for dust relative to solar and B-star abundances. Snow & Witt (1996) derive a new reference abundance which is a compilation of B, F and G stars abundances. The main difference between these models lies in the amount of iron contained in the dust phase which is higher (with respect to silicon) for the new reference abundance of Snow & Witt than for solar or B-star abundances. Independently of the adopted reference abundance, the dust composition in the two protostars seems deficient in magnesium and iron compared to silicon (Fe represents from 35 to 65% and 80% of the silicon for RAFGL7009S and IRAS19110 respectively and Mg represents $\sim$50% of the silicon for both sources). The remaining iron and magnesium could be in the gas phase or in a solid phase that has no observable transitions in the infrared. However such material, whatever it is made of, may be observable at other wavelengths.

Table 2. Comparison between silicates around RAFGL7009S and IRAS 19110 and interstellar and circumstellar silicates

	$\lambda_{10\mu m}$ (μm)	FWHM$_{10\mu m}$ [(1)] (μm)	(10/18) μm
MW Her[(2)]	9.8	2.8	5.7
warm O-deficient circum. sil.[(3)]	10	2.7	2.8
cool O-rich ISM sil.[(3)]	10	2.7	2.17
GC Sgr A IRS7*	9.8	2.15	3.8
IRAS 19110	9.6	2.35	2.2
RAFGL7009S	9.6	2.35	$\geq$2.2

From top to bottom: sequence of evolution of the silicates from the new to the older ones. The lines separate the evolved stars, ISM and protostellar objects. [(1)] calculated once all spectra have been normalised to the optical depth of the 10 μm band of RAFGL7009S, ice absorptions have been substracted for RAFGL7009S and IRAS 19110, [(2)] Stencel et al. 1990, [(3)] Ossenkopf et al. 1992

7. Evolution of the silicates

Silicates around protostars represent the end product of the evolution of silicates that were formed around evolved stars. They were processed in the ISM through the effects of sputtering, evaporation, annealing, shattering etc. In this study we assume that the silicates around RAFGL7009S and IRAS 19110 are representative of the silicate dust around massive protostars. Our study is consistent with that of Dorschner et al. (1995) who also found that the silicates around protostars are primarily pyroxenes, however, further studies are needed to verify this assumption for a wider range of protostars. The silicate spectra of these two sources do not match the ISM silicate spectra or those of evolved stars. This may indicate that the silicates have undergone transformation during the infall of the molecular cloud and star formation.

A first step in studying such processing is to compare the spectral characteristics of the silicate features at different stages of their evolution. We have therefore compared the silicate spectra of the two protostars studied in this paper with those of dense and "new" ISM. For the dense ISM we have used the data toward GC Sgr A* IRS7, and for "new" ISM we adopt the cool O-rich interstellar silicate data of Ossenkopf et al. (1992) which is derived from observations of the shells of OH/IR stars. We also compare the protostellar spectra with those derived for the O-deficient circumstellar silicates around evolved stars (Ossenkopf et al. 1992) and with the evolved star MW Her which shows pronounced silicates features (Stencel et al. 1990). The spectral characteristics of the different sources are displayed in Table 2. When comparing these spectral characteristics one must not forget that their determination requires some assumptions (modelling of the emission, determination of the continuum, etc.) that introduce uncertainties.

Several trends in the spectral evolution of silicates can be seen. First, the peak wavelength of the stretching mode of the silicates decreases from evolved stars to protostars. Second, the

FWHM of the stretching mode is wider in protostars than in GC Sgr A* IRS7 but narrower than around O-rich stars or in "new" ISM. Finally, the 10/18 μm band ratio seems to decrease from evolved stars to protostars. The last two points are in agreement with the theory of the evolution of silicates of Nuth & Hecht (1990). They found that the 10/18 μm band ratio is a tracer of the evolution of silicates and that it decreases during the processing of silicates. They also predicted that the processing of silicate grains in the ISM should tend to make them glassy and less chaotic than around evolved stars. The spectral signature of this phenomenon being the narrower 10 μm silicate band in the ISM compared to silicates around evolved stars. This band is broader in protostars than in the dense ISM (GC Sgr A* IRS7). This could be due to the coagulation of the grains during the collapse of the molecular cloud during star formation. Disordering of the glassy silicate state should also broaden the bands. However, the nature of the processes that lead to disordering of the silicates are uncertain and are less clear than the effects of coagulation.

The behaviour of the peak position of the 10 μm silicate band is more difficult to explain. Around evolved stars and in the ISM, the position is close to that of olivine (9.7–10 μm). In protostars the band peaks at 9.6 μm and we identify the silicates with pyroxene. Under the effects of annealing amorphous minerals tend to reorder themselves into a crystalline structure. As this transformation occurs, narrow bands appear in the infrared spectra of the mineral in the place of the broad amorphous bands. At the beginning of this process, before any structure appears, the amorphous bands can be shifted and broadened. Laboratory data on annealing do not agree with the evolution of the band position. Koike & Tsuchiyama (1992) find that the 10 μm band of olivine is shifted towards shorter wavelengths and the 18 μm band towards longer wavelengths whereas others report the reverse behaviour (Nuth & Donn 1982, Hallenbeck et al. 1998). Hallenbeck et al. (1998) report that during the annealing of Fe-silicate smokes, the stretching mode is shifted towards shorter wavelengths and that the evolution of Mg-Fe-silicates resembles that of Mg-silicates. As silicates are likely to be ferrous and "dirty", with inclusions of various oxides, more data concerning the annealing of iron containing silicates are needed. The decrease in the wavelength of the stretching mode of silicates could reflect a change in their composition. The conversion of olivine into pyroxene is possible and is dependant on the physical conditions (temperature of the mineral, redox character of the ambient medium, etc.). It requires some mechanisms that can displace the atoms and sufficient energy to re-order the SiO_4 tetrahedra. As an example the equilibrium $Mg_2SiO_4 + SiO_2 \rightleftharpoons 2\ MgSiO_3$ can be broken depending on the physical conditions. However, most of the reactions leading to structural changes in minerals have been studied at high temperatures where amorphous minerals should re-crystallise. This conversion is thus not straightforward in the amorphous state. Precise studies of the composition of silicates in various environments are needed in order to ascertain if there is indeed a general trend in the chemical and physical evolution of the silicates in the ISM and circumstellar environments.

In this study, we have not considered the later stages of protostellar evolution such as Herbig AeBe stars and disk-like stars. In these objects in which some of the silicates have crystallised, the amorphous silicate component is identified with olivine-type silicate (Malfait et al. 1998, Waelkens et al. 1996). This indicates that the silicates, in these objects, have undergone some processing. The nature of this processing is not yet fully understood.

8. Crystalline component

Interstellar grains undergo processing in the ISM and during the collapse of molecular clouds but this is not enough to crystallise them. We have determined an upper limit to the crystalline component of silicates (by mass) by assuming that all the grains are cold (T$\sim$20–40 K) and thus do not emit but only absorb at 10 μm. We then added crystalline olivine (containing 80% of magnesium) absorption to the 10 μm amorphous band and set an upper limit when the crystalline structure appears on the structureless amorphous band. We estimate the integrated absorption cross-section of the 10 μm band of the crystalline olivine to be $\sim 4.2\times 10^{-16}$ cm/molecule. We thus find that both objects contain no more than $\sim$1–2% of crystalline silicates. However one must note that this upper limit could be underestimated because we do not take into account radiative transfer effects. If there is indeed crystalline silicate around these protostars, this limit may then represent the maximum amount of crystalline silicate present in the ISM. The grains in the ISM are extremely cold and this component will be unobservable unless the grains are heated enough to emit in the 20–80 μm range where emission bands could be observed.

9. Conclusion

We have modelled the silicate features of two protostars RAFGL7009S and IRAS 19110+1045. These sources have deep silicate absorptions peaking at 9.6 and 18 μm. The bands correspond to amorphous pyroxene-type silicates rather than olivine. We cannot reproduce the spectra with compact laboratory pyroxenes. The addition of porosity and oxides is necessary to reproduce the features. About 15% (by volume) of vacuum is needed to account for the width of the 9.6 μm band, iron oxides permit a good fit to the 18 μm band, and aluminium can account for the 12–16 μm plateau. Aluminium incorporated into the structure of aluminosilicates gives a better fit than aluminium in Al_2O_3. Less silicon (relative to hydrogen) than available is needed to reproduce the silicate feature of the two sources. According to our model, about 35 to 80% of iron relative to silicon is contained in the refractory part of the dust grains around the two protostars. We believe that in the ISM and during the formation of protostars, the silicates undergo further processing that modifies their properties and thus their infrared spectra (both bands broaden, the 12–16 μm plateau is more pronounced, and the 10 μm band is slightly shifted towards shorter wavelengths). This processing is not sufficient to crystallize the silicates. We do not observe any structure in the silicate bands of either source

that could be the signature of crystalline silicates. We estimate that no more than 1–2% (by mass) of the silicates could be crystalline in either sources.

Acknowledgements. We thank J. Nuth for fruitful discussions. A.P. Jones is grateful to the Société de Secours des Amis des Sciences for funding during the course of this work.

References

Barlow M.J., 1978a, MNRAS 183, 367
Barlow M.J., 1978b, MNRAS 183, 397
Begemann B., Henning Th., Mutschke H., Dorschner J., 1995, Planet. Space Sc. 43, 1257
Begemann B., Dorschner J., Henning Th., et al., 1997, ApJ 476, 199
Bohren C. F., Huffman D. R., 1983, In: Absorption and Scattering of Light by Small Particles. John Wiley, New York
Bradley J.P., Sandford S.A., Walker R.M., 1988, In: Kerridge J.F., Matthews M.S. (eds.) Meteorites and the Early Solar System. 861
Dartois E., Cox P., Roelfsema P.R., et al., 1998a, A&A 338, L21
Dartois E., d'Hendecourt L., Boulanger F., et al., 1998b, A&A 331, 651
Dartois E., Schutte W., Geballe T.R., et al., 1999, A&A 342, L32
Dorschner J., Begemann B., Henning Th., Jager C., Mutschke H., 1995, A&A 300, 503
Gehrz R.D., 1989, In: Allamandola L.J., Tielens A.G.G.M. (eds.) Interstellar Dust. Kluwer, Dordrecht, 445
Guélin M., Lucas R., Cernicharo J., 1993, A&A 280, L19
d'Hendecourt L.B., Jourdain de Muizon M., Dartois E., et al., 1996, A&A 315, L365
Hallenbeck S.L., Nuth III J.A., Daukantas P.L., 1998, Icarus 131, 198
Henning Th., Mutschke H., 1997, A&A 327, 743
Henning Th., Begemann B., Mutschke H., Dorschner J., 1995, A&AS 112, 143
Howk J.C., Savage B.D., 1998, AAS Meeting 192, 4006H
Hunter T.R., 1997, Ph.D. Thesis, Caltech
Hunter T.R., Phillips T.G., Menten K.M., 1997, ApJ 478, 283
Jäger C., Mutschke H., Begemann B., Dorschner J., Henning Th., 1994, A&A 292, 641
Jones A.P., 1988, MNRAS 234, 209
Jones A.P., 1990, MNRAS 245, 331
Jones A.P., Tielens A.G.G.M., Hollenbach, 1996, ApJ 469, 740
Klotz A., Marty P., Boissel P., et al., 1995, A&A 304, 520
Koike C., Tsuchiyama A., 1992, MNRAS 255, 248
McCutcheon W.H., Sato T., Pyrton C.R., Matthews H.E., Dewdney P.E., 1995, AJ 110, 1762
Malfait K., Waelkens C., Waters L.B.F.M., et al., 1998, A&A 332, L25
Mutschke H., Begemann B., Gürtler J., et al., 1998, A&A 333, 188
Nuth III J.A., 1988, In: Bussolettiet E., et al. (eds.) Exp. Cosmic Dust Analogs. 191
Nuth III J.A., 1996, In: Greenberg J.M. (ed.) The Cosmic Dust Connection. Kluwer, Dordrecht, 205
Nuth III J.A., Donn B.D., 1982, ApJ 257, L103
Nuth III J.A., Hecht J.H., 1990, Ap&SS 163, 79
Ossenkopf V., Henning Th., Mathis J.S., 1992, A&A 261, 567
Pollack J.B., Beckwith S., Simonelli D.P., Roush T., Fong W., 1994, ApJ 421, 615
Rietmeijer F.J.M., Nuth III J.A., 1990, LPSC XXI, 1017
Savage B.D., Sembach K.R., 1996, ARA&A 34, 279
Sedlmayr E., 1989, In: Allamandola L.J., Tielens A.G.G.M. (eds.) Interstellar Dust. Kluwer, Dordrecht, 467
Serra G., Chaudret B., Saillard Y., et al., 1992, A&A 260, 489
Snow T.P., Witt A.N., 1996, ApJ 468, L65
Stencel R.E., Nuth III J.A., Little-Marenin I.R., Little S.J., 1990, ApJ 350, L45
Waters L.B.F.M., Molster F.J., de Jong T., et al., 1996, A&A 315, L361
Waters L.B.F.M., Beintema D.A., Zijlstra A.A., et al., 1998, A&A 331, L61
Waelkens C., Waters L.B.F.M., de Graauw M.S., et al., 1996, A&A 315, L245
Willner S.P., Gillet F.C., Herter T.L., et al., 1982, ApJ 253, 174
Ziurys L.M., Apponi A.J., Guélin M., Cernicharo J., 1995, ApJ 445, L47